

REPORT DOCUMENTATION PAGE			Form Approved OMB No. 0704-0188		
Public reporting burden for this collection of information is estimated to average 1 hour per response, including the time for reviewing instructions, searching existing data sources, gathering and maintaining the data needed, and completing and reviewing this collection of information. Send comments regarding this burden estimate or any other aspect of this collection of information, including suggestions for reducing this burden to Department of Defense, Washington Headquarters Services, Directorate for Information Operations and Reports (0704-0188), 1215 Jefferson Davis Highway, Suite 1204, Arlington, VA 22202-4302. Respondents should be aware that notwithstanding any other provision of law, no person shall be subject to any penalty for failing to comply with a collection of information if it does not display a currently valid OMB control number. PLEASE DO NOT RETURN YOUR FORM TO THE ABOVE ADDRESS.					
1. REPORT DATE (DD-MM-YYYY) January 2015		2. REPORT TYPE Technical Paper		3. DATES COVERED (From - To) January 2015-May 2015	
4. TITLE AND SUBTITLE X-ray Fluorescence Measurements of Turbulent Methane-Oxygen Shear Coaxial Flames			5a. CONTRACT NUMBER In-House		
			5b. GRANT NUMBER		
			5c. PROGRAM ELEMENT NUMBER		
6. AUTHOR(S) S.A. Schumaker, A.L. Kastengren, S.D. Danczyk, M.L. Lightfoot			5d. PROJECT NUMBER		
			5e. TASK NUMBER		
			5f. WORK UNIT NUMBER Q0BG		
7. PERFORMING ORGANIZATION NAME(S) AND ADDRESS(ES) Air Force Research Laboratory (AFMC) AFRL/RQRC 10 E. Saturn Blvd. Edwards AFB, CA 93524-7680			8. PERFORMING ORGANIZATION REPORT NO.		
9. SPONSORING / MONITORING AGENCY NAME(S) AND ADDRESS(ES) Air Force Research Laboratory (AFMC) AFRL/RQR 5 Pollux Drive Edwards AFB CA 93524-7048			10. SPONSOR/MONITOR'S ACRONYM(S)		
			11. SPONSOR/MONITOR'S REPORT NUMBER(S) AFRL-RQ-ED-TP-2015-095		
12. DISTRIBUTION / AVAILABILITY STATEMENT Distribution A: Approved for Public Release; Distribution Unlimited.					
13. SUPPLEMENTARY NOTES Technical paper presented at 9th US National Combustion Meeting, Cincinnati, Ohio, 17 May 2015. PA#15144					
14. ABSTRACT The use of x-ray fluorescence to make quantitative mixing field measurements in high temperature flames is attractive due to a number of positive attributes of x-ray fluorescence physics, particularly insensitivity to chemical bonding (which results in tracers being conserved in the flame) and negligible beam steering effects. To demonstrate the use of x-ray fluorescence in high temperature flames, the technique was applied to turbulent methane-oxygen shear coaxial flames. These flames are directly applicable to the oxygen-enriched combustion that occurs in liquid rocket engines where, due to the high temperature, it is difficult to obtain quantitative mixing field measurements using conventional optical diagnostics. The use of argon and krypton as x-ray fluorescence flow tracers was explored. Krypton was shown to require fewer corrections than the argon; background argon signal subtraction and signal trapping corrections were required. To allow tracking of both the fuel and oxidizer stream, cases were run where the tracer element was moved from the oxygen stream to the fuel stream. Comparison of the fuel traced and oxygen traced cases are compared to build a more complete picture of the reacting flow field. Results clearly demonstrate the ability of x-ray fluorescence to obtain quantitative measurements of projected density in high temperature flames. This work represents the first use of x-ray fluorescence to make quantitative tracer projected density measurements in turbulent flames.					
15. SUBJECT TERMS					
16. SECURITY CLASSIFICATION OF:			17. LIMITATION OF ABSTRACT SAR	18. NUMBER OF PAGES 12	19a. NAME OF RESPONSIBLE PERSON Stephen Schumaker
a. REPORT Unclassified	b. ABSTRACT Unclassified	c. THIS PAGE Unclassified			19b. TELEPHONE NO (include area code) 661-525-5165

9th U. S. National Combustion Meeting
Organized by the Central States Section of the Combustion Institute
May 17-20, 2015
Cincinnati, Ohio

X-ray Fluorescence Measurements of Turbulent Methane-Oxygen Shear Coaxial Flames

S. Alexander Schumaker^{1}, Alan L. Kastengren², Stephen Danczyk¹,
Malissa Lightfoot¹*

*¹Rocket Propulsion Division, Air Force Research Laboratory
Edwards AFB, CA 93536 USA*

*²X-ray Science Division, Advanced Photon Source Argonne National Laboratory
Argonne, IL 60439 USA*

**Corresponding Author Email: stephen.schumaker.1@us.af.mil*

Abstract: The use of x-ray fluorescence to make quantitative mixing field measurements in high temperature flames is attractive due to a number of positive attributes of x-ray fluorescence physics, particularly insensitivity to chemical bonding (which results in tracers being conserved in the flame) and negligible beam steering effects. To demonstrate the use of x-ray fluorescence in high temperature flames, the technique was applied to turbulent methane-oxygen shear coaxial flames. These flames are directly applicable to the oxygen-enriched combustion that occurs in liquid rocket engines where, due to the high temperature, it is difficult to obtain quantitative mixing field measurements using conventional optical diagnostics. The use of argon and krypton as x-ray fluorescence flow tracers was explored. Krypton was shown to require fewer corrections than the argon; background argon signal subtraction and signal trapping corrections were required. To allow tracking of both the fuel and oxidizer stream, cases were run where the tracer element was moved from the oxygen stream to the fuel stream. Comparison of the fuel traced and oxygen traced cases are compared to build a more complete picture of the reacting flow field. Results clearly demonstrate the ability of x-ray fluorescence to obtain quantitative measurements of projected density in high temperature flames. This work represents the first use of x-ray fluorescence to make quantitative tracer projected density measurements in turbulent flames.

Keywords: *X-ray, Fluorescence, Turbulent Flame, Shear Coaxial*

1. Introduction

X-ray diagnostics are an alternative to laser diagnostics and have a number of advantages for studying aerospace engine-relevant combustion fields. X-ray diagnostics have been used extensively to study multiphase nonreacting flow fields [1-4]. The most promising x-ray diagnostic for the study of turbulent flames is x-ray fluorescence. X-ray fluorescence has several advantages over fluorescence in the optical regime. X-ray fluorescence operates on the inner electron shells of atoms and is therefore insensitive to chemical bonding. This insensitivity to chemical bonding means that the species is conserved, even in reacting flowfields. Also, this interaction with inner shell electrons means that x-ray fluorescence is insensitive to pressure, temperature and surrounding species except for their impact on the local density. The photon energy of the exciting x-ray beam is flexible, with the beam energy only needing to be higher than the photon energy of the relevant absorption edge. This means that multiple tracers can be

excited at the same time if an overlapping region exists. X-ray fluorescence also has the same benefits as x-ray diagnostics in general such as a lack of refraction and beam-steering effects. Since the fluorescence signal is in the x-ray regime, no filtering of visible radiation from the flame or soot is required.

X-ray diagnostics, including x-ray fluorescence, also have some significant drawbacks, however. Practical measurements require a high flux synchrotron x-ray source and complex and expensive optics. The need for a synchrotron source means an experiment has to be brought to a fixed dedicated synchrotron x-ray. Another drawback is that, due to the fluxes and detectors currently available, measurements are either point or pathlength integrated and limited to acquisition rates less than 100 Hz. Additional details on the x-ray fluorescence technique can be found in references [5, 6]. Despite these disadvantages, x-ray fluorescence shows significant promise in making time averaged concentration and mixture fraction type measurements in single-phase and multiphase reacting flowfields.

Under this effort the use of x-ray fluorescence to make quantitative integrated concentration measurements (tracer projected density) in high-temperature single-phase flames was demonstrated. This technique was applied to methane/oxygen shear coaxial jet flames. This flame was chosen for a number of reasons. The shear coaxial jet injector is a typical injector design in liquid rocket engines, used as the main chamber element for Space Shuttle Main Engine [7], and has been used in the past as a unit physics problem for rocket combustion [8]. The high temperature nature of this flame makes quantitative measurements of tracer concentration and mixture fraction extremely difficult using optical diagnostics. The high, shear driven mixing of this configuration allows for a compact fully turbulent flame, which is readily incorporated into synchrotron beamline and allows for decreased data collection time. The use of two noble gas tracers, argon and krypton, was explored for the independent tracking of both the fuel and oxidizer streams. Results obtained under this effort clearly demonstrate the ability of x-ray fluorescence to make quantitative concentration measurements in propulsion relevant flames that require minimal corrections.

2. Methods / Experimental

The experimental effort was designed around two primary goals, demonstrate the ability to make quantitative measurements in high-temperature turbulent flames and obtain first-of-their-kind mixing data in flames relevant to liquid rocket engines. A methane/oxygen shear coaxial jet flame was chosen to meet those goals. The differences between a jet flame and a shear coaxial flame include the interaction between two shear layers in the near field of shear coaxial jets (versus one in a jet flame) and the reverse propellant orientation where the oxidizer is surrounded by the fuel. The high temperature nature of this flame makes quantitative measurements of concentration and mixture fraction difficult using typical optical diagnostics. In typical optical diagnostics the tracer reacts/dissociates at the high temperature of the chosen flames. Also, the high shear driven mixing of this configuration allowed for a compact fully turbulent flame.

The shear coaxial burner used in this study was designed to ensure fully turbulent combustion at Reynolds numbers greater than 10,000, allow testing at multiple momentum flux ratio conditions (primary controller of mixing in shear coaxial jets), and minimize mass flow rates (decrease the amount of propellant required to run the experiment). Sizing of the burner was based on the dissertation work of the principal investigator [8]. A single burner geometry was used in this study. A coflow of nitrogen was placed around the flame to eliminate combustion of the methane with the sounding air and to reduce the background argon signal

caused by the naturally occurring argon in the air. A Kapton-film box was added around the burner to further decrease the background argon signal. A solid model (including dimensions) and picture of the burner used are shown as Fig. 1.

Measurements were conducted at the 7-BM beamline of the Advanced Photon Source (APS) at Argonne National Laboratory [9], one of the world's largest and brightest synchrotron light sources. An x-ray beam $5 \times 6 \mu\text{m}$ in size FWHM (divergence approximately $1.5 \times 2.5 \text{ mrad}$) was

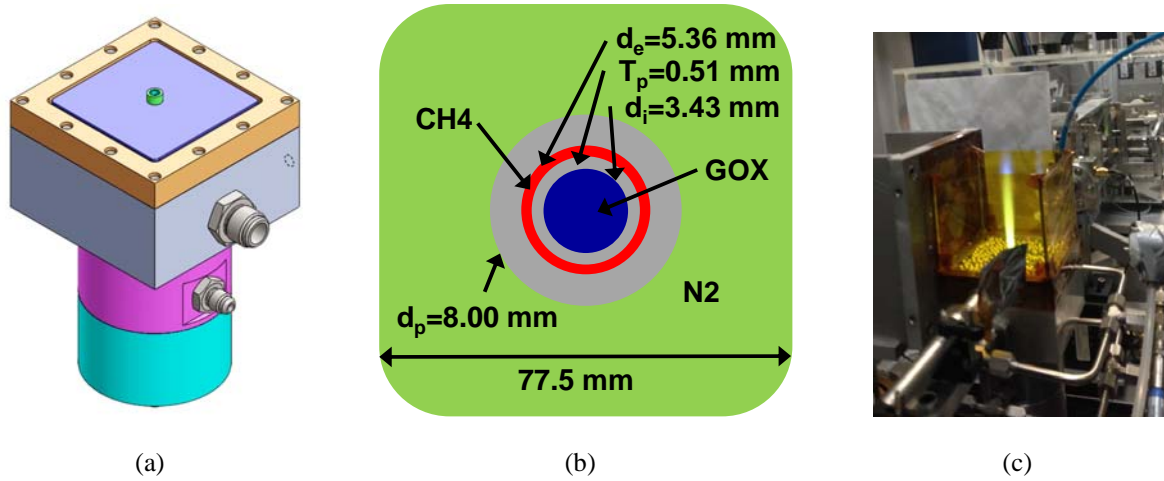


Figure 1: (a) Model of the shear coaxial burner used in the current study. (b) Representation of the injector tip of the shear coaxial burner with propellant streams and dimensions labeled. (c) Picture of flame during testing at APS with Kapton shield.

used to illuminate the flame. A biased diamond-based transmission photodiode was used to monitor the incident beam intensity, with a biased Si-PIN diode used to collect the transmitted x-ray beam intensity. A silicon drift diode (SDD) energy-dispersive detector was used to collect fluorescence photons, with the SDD placed 125 mm from the flame. To minimize the elastic scattering encountered by the SDD, it was placed at 90° to the incident beam in the horizontal plane. A sketch of the x-ray fluorescence experimental setup is shown in Fig. 2.

Since the elements commonly present in flames (H,C,N,O) do not undergo x-ray fluorescence at useful photon energies, fluorescence is induced by the addition of fluorescence tracer gases. Two tracers are used in this study: Ar and Kr. Various properties of the tracers are given in Table 1. Both gases, being inert, will have little impact on the flame, other than dilution. Argon has the advantage of being closer in atomic mass to other species in the flame, limiting differential diffusion. It is also easy to excite and low-cost. Krypton is, by most measures, a superior tracer: it has higher fluorescence efficiency, the fluorescence emission is at higher energy, meaning the effects of signal trapping will be greatly reduced, and the concentration within the air is too low to be detected, so that there is no background signal to subtract.

To perform the measurements, the flame is positioned with respect to the x-ray beam, the absorption and fluorescence signals are collected for 1-2 s, and the flame is repositioned for another measurement location. Each measurement (both for absorption and fluorescence) is a pathlength-integrated measurement along the incident x-ray beam path. To probe the entire

flowfield, a series of scans transverse to the flame axis were performed, resulting in a two-dimensional raster-scan measurement of the flame. The raster-scan measurements are then interpolated to create a projected image of the flame (Fig. 3).

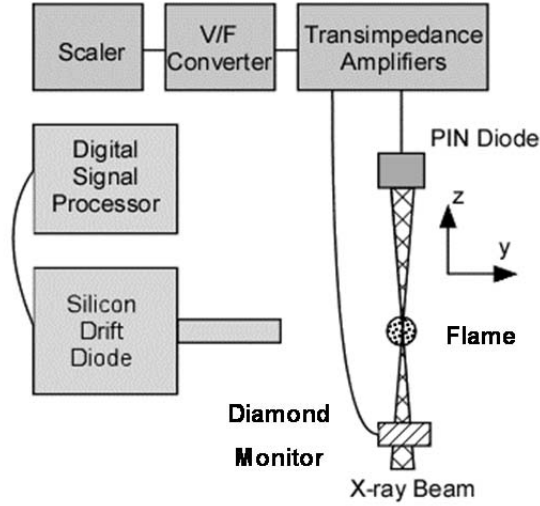


Figure 2: Sketch of the x-ray fluorescence experimental setup

Table 1: Tracer properties

	Ar	Kr
Atomic Mass (amu)	39.95	83.80
Threshold Energy, keV	3.21	14.33
Fluorescence Energy, keV	3.0, 3.2	12.6, 14.1
Fluorescence Efficiency	0.12	0.62

One disadvantage of x-ray diagnostics is the need for a synchrotron x-ray source. Synchrotron x-ray sources such as APS typically lack fluid delivery infrastructure found in combustion and fluid mechanics laboratories. To overcome this deficit a propellant delivery cart was designed and built for this effort. This cart has three propellant delivery systems and operates off standard k-bottles. Two of the propellant delivery systems are for the main propellants, methane and oxygen. The third is for a tracer gas. The third system has a three-way valve which allows the tracer gas to be mixed into either the oxidizer or fuel stream. Flow rates were measured using sonic nozzles and high accuracy pressure transducers. The system has the ability to be operated remotely since no one can be in the hutch when the beam is active. To aid in the remote operation and to supply the nitrogen coflow this propellant delivery system was integrated with the Air Force Research Laboratories' (AFRL) Mobile Flow Laboratory (MFL). This facility is designed to allow aerospace-propulsion injector testing at remote diagnostic facilities that do not have the infrastructure to provide relevant flow conditions. Details on the MFL can be found in reference [10].

The data analysis required to convert x-ray transmission and raw fluorescence flux to a quantity of fluorescence tracer in the beam requires several steps. At each beam position, the x-ray intensity after the flame is normalized by the incident intensity. This corrected intensity is furthermore normalized by the intensity far outside of the flame, where the absorption is due to the ambient gas alone; this gives the x-ray transmission through the flame as a function of beam position. Finally, the Beer-Lambert law is used to convert this transmission to a measure of the density of material in the x-ray beam; at this stage, this quantity is left uncalibrated, simply as extinction lengths (i.e., $1/e$ pathlengths) of material in the beam. This quantity can be positive in regions where the gases absorb more strongly than the ambient air (e.g., cold argon-rich gas streams) and negative in regions where the flame absorbs x-rays less strongly than the ambient air (e.g., high-temperature regions, where the local gas density is quite low).

Following this normalization and conversion process, the fluorescence data has been corrected for variations in the incoming beam intensity, attenuation of the incident beam in the sample (using the radiography data as a measure of attenuation), and detector dead-time effects [11]. Aside from signal trapping corrections, the corrected fluorescence flux at the end of this stage of the data processing is proportional to the amount of fluorescence tracer in the beam. A cold-flow scan near the nozzle (where the jet appears to be a circle of constant density in cross-section) is used to calibrate the fluorescence signal to an amount of fluorescence tracer in the beam. Kr tracer cases use a cold flow scan at 0.25 mm and Ar tracer cases use a cold flow scan at 1.00 mm downstream of the nozzle exit for fluorescence signal calibration which were the closest points taken to the injector exit. The inner jet diameter plus the thickness of the injector post tip was chosen as the calibration pathlength to account for the post tip recirculation zones.

The final correction to the fluorescence data is to correct for signal trapping. The major steps for signal trapping corrections for each transverse scan are

1. Assuming that the underlying 2D distribution of fluorescence tracer is axisymmetric, perform a fit to the corrected fluorescence data, which represent a projection of the 2D distribution along the incident x-ray beam path.
2. Scale the corrected radiography signal from the incident photon energy (6.7 keV for Ar fluorescence, 14.7 keV for Kr fluorescence) to the fluorescence photon energy (3.0 keV for Ar, 12.6 keV for Kr).
3. Like with the fluorescence signal, perform a fit to the scaled radiography data, assuming the underlying 2D distribution is axisymmetric.
4. Compute the corresponding 2D distributions of fluorescence and absorption from the fits in steps 1 and 3.
5. For each point in the 2D fluorescence distribution, use the 2D absorption distribution to compute how much absorption will occur between the point and the fluorescence detector.
6. For each beam path through the 2D fluorescence distribution, determine the mean fluorescence signal trapping.
7. Use this estimated signal trapping to correct the fluorescence signal.
8. If necessary, iterate.

The signal trapping corrections are far different between the Ar and Kr fluorescence. The Kr fluorescence photon is at relatively high energy and encounters very little signal trapping ($< 1\%$). As such, signal trapping corrections were not performed on the Kr fluorescence data. For argon fluorescence, the fluorescence photon is at low energy (3.0 keV), and is strongly absorbed by air.

As such, the signal trapping corrections are quite large (up to $\sim 50\%$) even in this gas-phase flow. As such, the signal trapping corrections are essential here. Even with the large signal trapping corrections required for the Ar fluorescence data, one or two iterations of the signal trapping procedure were sufficient to achieve a converged solution for the signal trapping.

Test conditions were designed to explore the use of both Ar and Kr as tracers, track both the fuel and oxidizer stream, and directly compare reacting and nonreacting turbulent mixing. The Reynolds Number (Re) was kept above 10,000 to ensure turbulent combustion. The Re number definition used here is based on a theoretical jet with external jet fluid properties and a velocity that provides the same total momentum flux as the actual coaxial jet with the injector post thickness ignored, which is a common formulation for shear coaxial jets [12]. The momentum flux ratio (J) was varied between 5 and 10. The test conditions used in this report are provided in Table 2. Variables included in Table 2 include the fuel exit velocity (U_F), the oxidizer exit velocity (U_O), the coflow velocity (U_C), the fuel stream mass flow rate (\dot{m}_F), the oxidizer stream mass flow rate (\dot{m}_O), and the tracer mass fraction (Y_{Tracer}). Tracer mass flowrate is included in the appropriate propellant stream mass flow rate for each case. The tracer mass flowrate is also taken into account when calculating the propellant exit velocities. Note the oxidizer always flows from the center jet surrounded by an annulus of fuel.

Table 2: Test Matrix

Case	Tracer	Tracked Stream	Type	J	Re	U_F , m/s	U_O , m/s	U_C , m/s	\dot{m}_F , g/s	\dot{m}_O , g/s	Y_{Tracer}
J5KR	Kr	O2	Flame	5.09	14,000	54.6	17.2	0.80	0.261	0.213	0.073
J5MKR	Kr	CH4	Flame	6.54	10,000	41.2	11.9	0.98	0.221	0.127	0.073
J5CKR	Kr	O2	Cold	5.15	14,000	54.2	17.0	0.80	0.263	0.214	0.075
J5AR	Ar	O2	Flame	5.08	14,000	54.6	17.3	0.80	0.260	0.212	0.121
J8AR	Ar	O2	Flame	8.00	11,000	48.0	12.1	0.98	0.228	0.148	0.120
J10AR	Ar	O2	Flame	10.0	11,000	49.3	11.1	0.96	0.234	0.137	0.122

3. Results and Discussion

In an effort to demonstrate the use of x-ray fluorescence for making quantitative measurements in turbulent high temperature flames, conditions were chosen to explore the use of Ar and Kr as tracers, tracking both the fuel and oxidizer propellant streams and comparing reacting and nonreacting cases. Figure 3 shows projected Kr mass distribution plots for three Kr fluorescence cases. All plots are provided in terms of a projected density since the x-ray fluorescence measurements are pathlength integrated across the flow field; the plots are not a 2D concentration profile typically seen from planar laser fluorescence results.

Figure 3a shows a shear coaxial jet flame operating at J of 5.1 where 7.3% by mass of Kr was added to the inner jet oxygen stream. The general flame features that would be expected from a shear coaxial jet flame are seen in Fig. 3a. These features include a core region of oxygen (red and orange contours) which is rapidly consumed as the methane and oxygen progress downstream, mix, and combust as the mixture fraction approaches the stoichiometric value of 0.8. Outside of this core region, the Kr concentration quickly decreases as it is heated in the flame and transitions to tracking the low density hot products which further mix and diffuse with the outer methane stream and the nitrogen coflow. Well-formed conical shells can be seen

soundings the flame in Fig. 3a which indicate the extent to which the products have mixed with the outer gas streams. These contours nicely demonstrate the high signal-to-noise ratio of the Kr fluorescence as contours as low as 8 ng/mm^2 are resolved compared to the 370 ng/mm^2 at the center of the jet exit. One downside to tracking only a single propellant stream at a time is that the exact location of the flame is unclear. In future work both propellant streams will be tracked simultaneously allowing the location of the stoichiometric mixture fraction and, therefore, the flame to be located.

In Fig. 3b the Kr tracer was removed from the oxygen stream and placed in the methane stream. Figure 3b has a number of interesting features. Unlike the monotonically decreasing behavior observed when Kr is in the oxygen stream, when Kr is added to the fuel stream there are some locations where the projected density increases as the flame progresses downstream. The cause of this is increase or near constant projected density is twofold. The lesser of the two causes is that all of the test conditions are run fuel rich so excess methane in the annular jet mixes with the coflowing nitrogen. While this mixing does decrease the local concentration, as evident by the increasing methane projected density width, the decrease is significantly less than that caused by heating in the flame. The primary cause of this effect is the dependence of the projected density on the flow velocity. Over a pathlength with uniform flow properties the projected density is proportional to the local tracer mass flux divided by the velocity. So as the methane moves downstream and mixes with the coflow, the velocity decreases resulting in the increase in projected density even as the flow field widens. This velocity dependence is also evident at the jet exit where the low projected density at the center of the jet is due to the high fuel stream exit velocity which rapidly decelerates as the fuel mixes with the significantly slower inner jet and coflow.

An advantage of the x-ray fluorescence diagnostic is that the same measurement technique can be applied to both reacting and nonreacting cases without making changes. Figure 3c shows a nonreacting shear coaxial jet with a J of 5. This test condition is identical to the reacting case shown in Fig. 3a except in this case the flow is not combusting. As expected, a comparison of the reacting (Fig. 3a) and nonreacting cases (Fig. 3b) shows significantly faster mixing (faster decrease in projected density) in the nonreacting case. The decreased mixing in the reacting case is a result of reduced mass entrainment due to low density surrounding the flame located between the two propellant streams. This ability to make identical measurements between reacting and nonreacting flowfield could be used to measure the difference in mass entrainments without having to use scaling constants to compare results from different reacting and nonreacting measurement techniques [13].

Ar fluorescence results are shown in Fig. 4 for oxygen tracked reacting cases at three different momentum flux conditions. Figure 4 shows the expected trend of a decrease in core length and flame length with increasing momentum flux ratio; such an effect has been well documented [7]. The test condition in Fig. 4a with Ar as the tracer is very close to the test condition shown in Fig. 3a with Kr as the tracer. As expected, the length and size of the core region between these two conditions is similar. However, differences between the Ar and Kr tracked cases are observed related to the signal to noise and the background interference. The conical shells that could be seen soundings the flame when Kr is added are largely lost in the Ar fluorescence contour plot. A higher projected density region at the top of the Ar case (Fig. 4a) is likely caused by entrainment of room air over the Kapton-film shield resulting in an increase in the Ar background signal. This entrainment of room air over the Kapton film appears to decrease

as the flame shortens in the higher J cases, shown in Fig. 4b and 4c. The decreased data quality seen in the Ar fluorescence results compared to the Kr results are a consequence of lower signal strength and higher background noise from the Ar fluorescence. The lower signal strength of the Ar occurs because the fluorescence efficiency is significantly lower and due to the signal lost to signal trapping. For the results presented here, Kr is the superior tracer. While Kr was the better tracer, these results show that both Ar and Kr are acceptable tracers for the study of gaseous turbulent flames. Argon should not be discounted as a useful tracer, however, since it would have an advantage in flow fields where diffusion was important with an atomic mass closer to the other species in the flame. With the high signal-to-noise ratio of the Kr data, the Kr mass fraction can likely be decreased from the 7 % used here to 2 or 3 % in future work.

4. Future Work

Now that the use of x-ray fluorescence for obtaining quantitative integrated tracer concentration measurements in turbulent flames has been demonstrated, a number of refinements to the technique and the characterization of increasingly complex flames should be pursued. One unmet goal of this current effort was the measurement of the mixture fraction field. To measure mixture fraction both propellant streams need to be tracked simultaneously. Two-dimensional concentration fields can then be obtained using an Abel Inversion of the axisymmetric projected density data for both streams from which mixture fraction can be measured. The current work has shown that both Ar and Kr are acceptable gas phase tracers and the silicon drift diode used to detect the fluorescence signal captures a complete x-ray spectrum allowing the Ar and Kr signals to be separated. However to excite both tracers at the same time the 7-BM beamline, where these tests are conducted, must be upgraded with either a new multilayer monochromator reflector to allow to allow two photo energies (7 & 15 keV) or to allow “white beam” (broad spectrum beam) into the test hutch. Both of these upgrades are currently being explored. Another upgrade to the measurement technique would be the use of a polycapillary optic which would allow the measurement of x-ray fluorescence at a point instead of pathlength integrated measurements, making the use of an Abel inversion unnecessary. A point technique would be better able to deal with asymmetry but would require significantly more measurements to build an overall flame profile.

In addition to improving the x-ray fluorescence measurement technique for flames, the technique should be applied to increasingly difficult to interrogate propulsion relevant flames. One of the major strengths of x-ray diagnostics is the lack of reflections at density interfaces which makes them ideal for obtaining measurements in multiphase flowfields. Because of the multireflection issue in dense spray flames, there is a lack of quantitative data in the literature. X-ray fluorescence is ideal for making the quantitative measurements necessary to validate spray combustion models. This technique is also not affected by changes in pressure or by the phase change between subcritical and supercritical fluids making it ideal to investigate changes in flame structure due to phase changes.

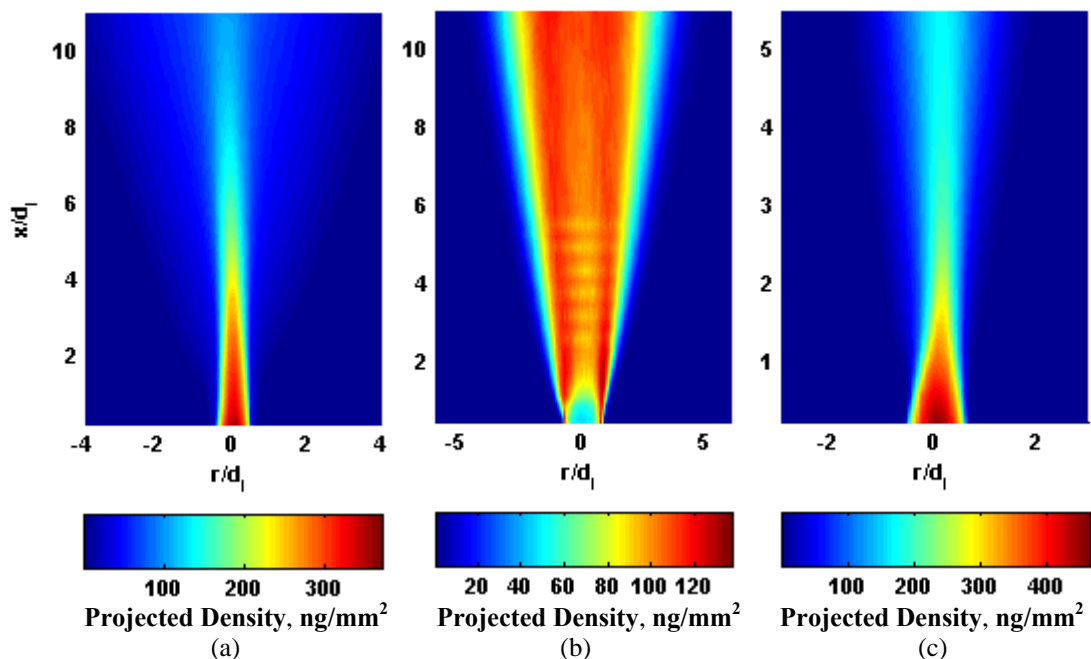


Figure 3: Kr fluorescence contour plots of projected density in ng/mm^2 for (a) O2 tracked reacting case J5KR, (b) CH4 tracked reacting case J5MKR, and (c) O2 tracked nonreacting case J5CKR.

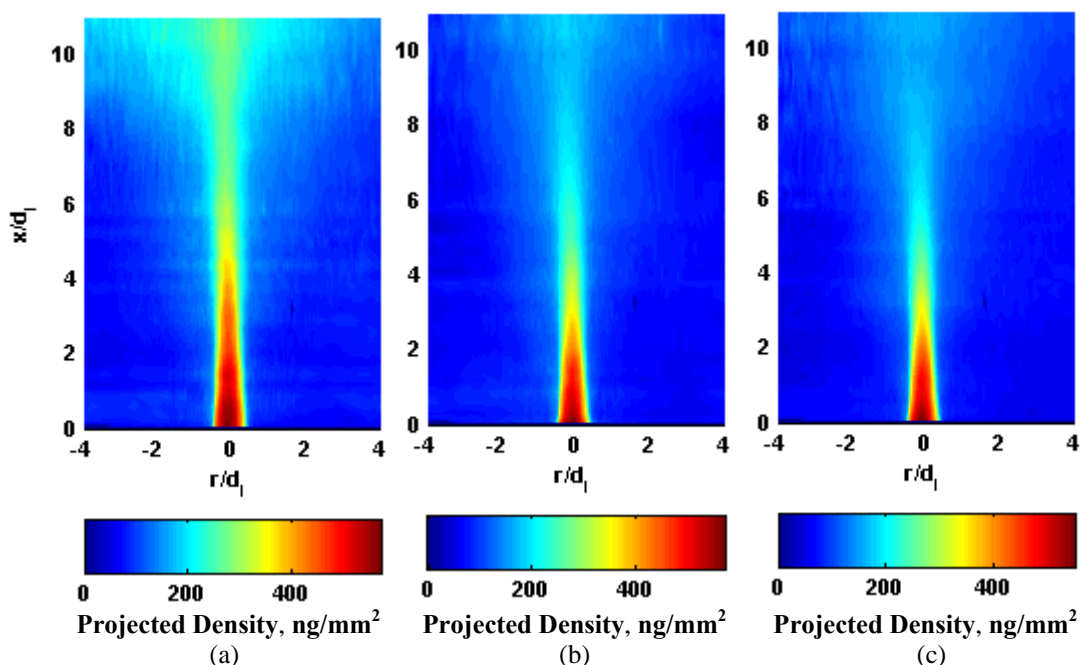


Figure 4: Ar fluorescence contour plots of projected density in ng/mm^2 for O2 tracked reacting cases (a) J5AR, (b) J8AR, and (C) J10AR.

5. Summary & Conclusions

X-ray fluorescence was used to make first of their kind quantitative projected density measurements in high temperature turbulent shear coaxial jet flames. High flame temperatures were achieved through the burning of methane and oxygen. Test conditions were designed to explore the use of both Ar and Kr as tracers, track both the fuel and oxidizer streams, and directly compare reacting and nonreacting turbulent mixing. For the current study Kr was shown to be the better tracer due to its higher fluorescence efficiency, negligible signal trapping, and minimal background signal. However, both Ar and Kr were shown to be acceptable tracers for the study of gaseous turbulent flames. Results showed that x-ray fluorescence could successfully be used to track both the oxidizer and fuel streams of a flame, although due to current hardware limitations, this study did not measure both simultaneously. It was also shown the same x-ray fluorescence technique could be applied to a nonreacting or reacting flowfield allowing a direct measure of how combustion effects mixing. Future work should apply the x-ray fluorescence to increasingly relevant aerospace propulsion flames, including spray flames and simultaneous tracking of the fuel and oxidizer to obtain mixture fraction fields.

5. Acknowledgements

This research effort was made possible by the award of Air Force Research Laboratory Aerospace Systems Directorate Chief Scientist Innovation Research Funds (CSIRF). A portion of this research was performed at the 7-BM beamline of the Advanced Photon Source, Argonne National Laboratory. Use of the Advanced Photon Source at Argonne National Laboratory was supported by the U. S. Department of Energy, Office of Science, Office of Basic Energy Sciences, under Contract No. DE-AC02-06CH11357. The authors would like to thank Mr. Earl Thomas (ERC, Inc.) and Mr. Heath Mitchell (Jacobs Technology Inc.) for their assistance during the testing campaign at Argonne National Laboratory and Mr. Paul Rue (ERC, Inc.) for construction of the propellant delivery cart.

6. References

- [1] A.L. Kastengren, C.F. Powell, Z. Liu, S. Moon, J. Gao, X. Zhang, J. Wang, Axial Development of Diesel Sprays at Varying Ambient Density, 22nd Annual Conference on Liquid Atomization and Spray Systems, Cincinnati, Ohio (2010).
- [2] K.C. Lin, C. Carter, S. Smith, A. Kastengren, Exploration of Aerated-Liquid Jets Using X-Ray Radiography, 50th AIAA Aerospace Sciences Meeting, Nashville, Tennessee (2012).
- [3] B.R. Halls, T.J. Heindel, T.R. Meyer, A.L. Kastengren, X-ray Spray Diagnostics: Comparing Sources and Techniques, 50th AIAA Aerospace Sciences Meeting, Nashville, Tennessee (2012).
- [4] S.A. Schumaker, S.A. Danczyk, D.A. Lightfoot, and A.L. Kastengren, Interpretation of Core Lengths in Shear Coaxial Rocket injectors from X-ray Radiography Measurements, 50th AIAA Joint Propulsion Conference, Cleveland, Ohio (2014).
- [5] A.L. Kastengren, C.F. Powell, E.M. Dufresne, D.A. Walko, J Synchrotron Radiat, 18 (2011), doi:10.1107/S0909046511024435.
- [6] A.L. Kastengren, "X-Ray Fluorescence as a Gas-Phase Mixing Diagnostic," Spring Technical Meeting of the Central States Section of the Combustion Institute, Tulsa, Oklahoma (2014).

- [7] G.P. Sutton, O Biblarz, Rocket Propulsion elements 7th ed., John Wiley & Sons, New York (2001).
- [8] S.A. Schumaker, An Experimental Investigation of Reacting and Nonreacting Coaxial Jet Mixing in a Laboratory Rocket Engine, PhD Dissertation University of Michigan (2009).
- [9] A.L. Kastengren, C.F. Powell, D. Arms, E.M. Dufresne, H. Gibson, J. Wang, J Synchrotron Radiat, 19 (2012) 654-657.
- [10] S.A. Schumaker, S.A. Danczyk, M.L. Lightfoot, A.K. Kastengren, Interpretation of Core Length in shear Coaxial Rocket Injectors from X-ray Radiography, 50th AIAA Joint Propulsion Conference, Cleveland, Ohio (2014).
- [11] D.A. Walko, D.A. Arms, A. Miceli, A. Kastengren, Nucl. Instrum. Methods Phys. Res. A., 649 (2011) 81-83.
- [12] M. Favre-Marinet, E.B.Camano, J. Sarboch, Exp in Fluids, 26 (1999) 97-106.
- [13] K.M. Tacina, W.J.A. Dahm, J Fluid Mech, 415(2000) 23-44.